

RESEARCH ARTICLE

Reprimo tissue-specific expression pattern is conserved between zebrafish and human

Ricardo J. Figueroa¹, Gonzalo Carrasco-Avino^{2,3}, Ignacio A. Wichmann^{2,4}, Martin Lange⁵, Gareth I. Owen^{1,2,4,6,7}, Arndt F. Siekmann⁵, Alejandro H. Corvalán^{2,4,7}, Juan C. Opazo⁸, Julio D. Amigo^{1*}

1 Departamento de Fisiología, Facultad de Ciencias Biológicas, Pontificia Universidad Católica de Chile, Santiago, Chile, **2** Advanced Center for Chronic Diseases (ACCDiS), Santiago, Chile, **3** Pathology Department, Hospital Clínico Universidad de Chile, Santiago, Chile, **4** Departamento de Oncología y Hematología, Facultad de Medicina, Pontificia Universidad Católica de Chile, Santiago, Chile, **5** Max Planck Institute for Molecular Biomedicine, Muenster, Germany, **6** Millennium Institute on Immunology and Immunotherapy, Santiago, Chile, **7** Center UC for Investigation in Oncology (CITO), Pontificia Universidad Católica de Chile, Santiago, Chile, **8** Instituto de Ciencias Ambientales y Evolutivas, Facultad de Ciencias, Universidad Austral de Chile, Valdivia, Chile

☯ These authors contributed equally to this work.

* jamigo@bio.puc.cl



OPEN ACCESS

Citation: Figueroa RJ, Carrasco-Avino G, Wichmann IA, Lange M, Owen GI, Siekmann AF, et al. (2017) Reprimo tissue-specific expression pattern is conserved between zebrafish and human. *PLoS ONE* 12(5): e0178274. <https://doi.org/10.1371/journal.pone.0178274>

Editor: Marc Robinson-Rechavi, University of Lausanne, SWITZERLAND

Received: February 7, 2017

Accepted: May 10, 2017

Published: May 31, 2017

Copyright: © 2017 Figueroa et al. This is an open access article distributed under the terms of the [Creative Commons Attribution License](https://creativecommons.org/licenses/by/4.0/), which permits unrestricted use, distribution, and reproduction in any medium, provided the original author and source are credited.

Data Availability Statement: All relevant data are included within the paper and its Supporting Information files.

Funding: This work was funded by grants BMBF-CONICYT 20140027 to AFS and JDA, CONICYT-ANILLO ACT1402 and CRP-ICGEB CH15-01 to JDA, FONDECYT 1160627, to JCO, 1140970 to GIO, 1151411 to AHC, BMRC 13CTI-21526-P6, IMII P09/016-F and CONICYT-FONDAP 15130011 to GIO and AHC.

Abstract

Reprimo (RPRM), a member of the *RPRM* gene family, is a tumor-suppressor gene involved in the regulation of the p53-mediated cell cycle arrest at G2/M. *RPRM* has been associated with malignant tumor progression and proposed as a potential biomarker for early cancer detection. However, the expression and role of *RPRM*, as well as its family, are poorly understood and their physiology is as yet unstudied. In this scenario, a model system like the zebrafish could serve to dissect the role of the *RPRM* family members *in vivo*. Phylogenetic analysis reveals that *RPRM* and *RPRML* have been differentially retained by most species throughout vertebrate evolution, yet *RPRM3* has been retained only in a small group of distantly related species, including zebrafish. Herein, we characterized the spatiotemporal expression of *RPRM* (present in zebrafish as an infraclass duplication *rprma/rprmb*), *RPRML* and *RPRM3* in the zebrafish. By whole-mount *in situ* hybridization (WISH) and fluorescent *in situ* hybridization (FISH), we demonstrate that *rprm* (*rprma/rprmb*) and *rprml* show a similar spatiotemporal expression profile during zebrafish development. At early developmental stages *rprmb* is expressed in somites. After one day post-fertilization, *rprm* (*rprma/rprmb*) and *rprml* are expressed in the notochord, brain, blood vessels and digestive tube. On the other hand, *rprm3* shows the most unique expression profile, being expressed only in the central nervous system (CNS). We assessed the expression patterns of *RPRM* gene transcripts in adult zebrafish and human *RPRM* protein product in tissue samples by RT-qPCR and immunohistochemistry (IHC) staining, respectively. Strikingly, tissue-specific expression patterns of the *RPRM* transcripts and protein are conserved between zebrafish and humans. We propose the zebrafish as a powerful tool to elucidate the both physiological and pathological roles of the *RPRM* gene family.

Competing interests: The authors have declared that no competing interests exist.

Introduction

The *Reprimo* (*RPRM*) gene family has only been identified in vertebrates and that is composed by three paralogs: *RPRM*, *RPRML* and *RPRM3* [1]. This group of genes diversified during the two rounds of whole genome duplication that occurred early in the evolution of vertebrates. Following duplication, family members were differentially retained [1]. Thus, *RPRM* and *RPRML* have been retained in most vertebrates, including humans; whereas *RPRM3* has been retained only in a small group of distantly related species [1], including the zebrafish (Fig 1). Synteny analyses further confirmed that these copies were originated as a product of whole genome duplication, as genes found up- and down-stream conserved in both zebrafish copies were, to some extent, conserved S1 Fig. These genes are also conserved in the genomic location where the human *RPRM* gene is located S1 Fig.

To date, only the *RPRM* paralog has been studied. *RPRM* is a highly glycosylated cytoplasmic protein, involved in p53-induced cell cycle arrest at G2 through the regulation of the Cdc2-cyclin B1 complex activity by an as yet undiscovered G2/M checkpoint mechanism [2, 3]. *RPRM* has also been suggested as a p53-dependent putative tumor suppressor gene [3]. *In vitro* studies have shown that overexpression of *RPRM* results in reduced cell proliferation, migration and invasion [4, 5], as well as increased apoptosis [6]. *RPRM* is a potential class II (inactivation occurring by epigenetic mechanisms) tumor suppressor gene (TSG). Inactivation is driven principally by aberrant methylation of its promoter region [4, 7, 8] and correlates with genetic instability in human cancers, such as gastrointestinal tumors [9, 10]. In addition, aberrant methylation of its promoter region has been proposed as a biomarker for non-invasive detection of gastric cancer [7]. Interestingly, no literature exists on the presence or role of *Reprimo-like* (*RPRML*) protein in either physiology or pathophysiology.

Model organism

Comparative genomics have gained medical relevance, as further insights into animal genetics provide information about conservation between species and serve to develop new animal models to study human diseases [11, 12]. The zebrafish is a relevant model organism for the analysis of vertebrate development, and has become a popular organism for the study of human cancers [12]. Some advantages of this animal model include the transparency and complexity of the zebrafish embryos, combined with the easy-to-use and high-throughput features of *in vitro* models [13]. Additionally, many of the components that regulate angiogenesis and cancer are conserved between zebrafish and humans [14, 15]. Recently, we described the evolution of the *RPRM* protein family members among vertebrates and described three distinct gene lineages: *RPRM*, *RPRML* and *RPRM3* [1]. To date, no robust *in vivo* models exist to examine the temporal and spatial expression patterns of *RPRM* products during normal and pathological processes.

Herein, we characterize the temporal and spatial expression patterns of *RPRM* paralogs during vertebrate development *in vivo*, by the use of a zebrafish development model. We confirm that all three *RPRM* gene family members (*RPRM*, *RPRML* and *RPRM3*) have been retained, and are expressed in zebrafish. In the zebrafish, two copies of the *RPRM* orthologue are present, termed *rprma* and *rprmb*, which represent an infraclass duplication event within the teleost lineage. In zebrafish, *rprm* (*rprma*, *rprmb*) and *rprml* are expressed during central nervous system (CNS), blood vessel and digestive tube formation. To our knowledge, these data constitute the first evidence of *RPRM* gene family expression during embryonic development, including the recently described member of the gene family, *RPRM3*. Furthermore, we show that the expression pattern of the *RPRM* orthologue is conserved between zebrafish and humans. The strong conservation in *RPRM* gene expression patterns in various tissues

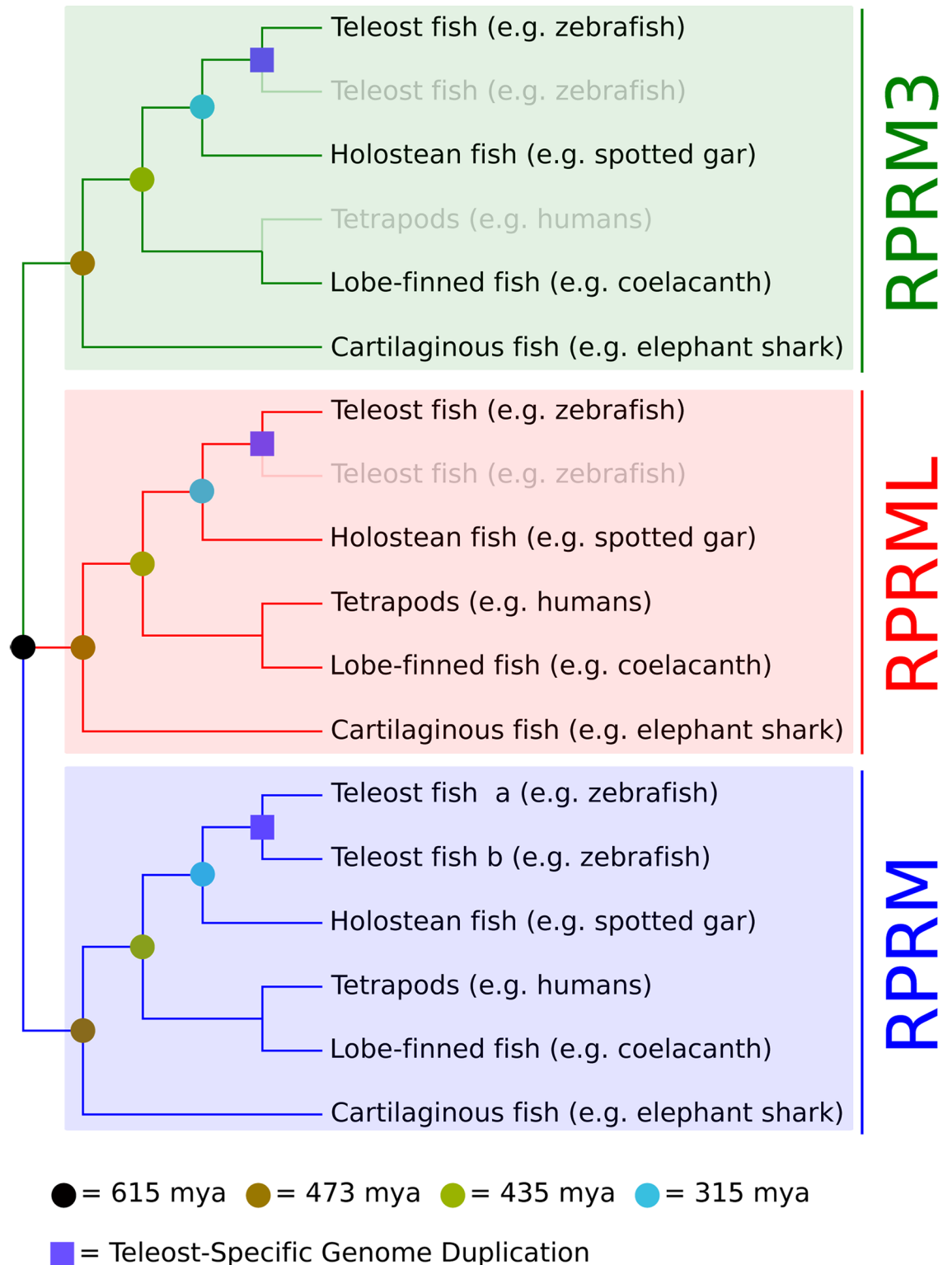


Fig 1. Evolutionary history of the *reprimo* gene family in gnathostome vertebrates. *Reprimo* genes (*RPRM*, *RPRML* and *RPRM3*) diversified as a product of the two rounds of whole genome duplication occurred in the last common ancestor of vertebrates. After that, they were differentially retained among the different group of vertebrates. Teleost fish (e.g. zebrafish) underwent an extra round of whole genome duplication that further expanded this group of genes, however, not all *reprimo* genes were retained in all species. Thus, teleost species retained duplicated copies only in the *RPRM* gene

lineage, while in the other two (*RPRML* and *RPRM3*), only one of them was retained. Diffuse lines represent gene lineages that are not retained in actual species. Divergence time estimates were obtained from the TimeTree public database [38]. The 615 mya estimates correspond to the last common ancestor of vertebrates.

<https://doi.org/10.1371/journal.pone.0178274.g001>

between fish and human, suggest that zebrafish may serve as a useful model organism to identify and study the function of *RPRM* genes in organismal development, as well as physiological and pathological processes.

Materials and methods

Multiple sequence alignment

In order to identify potential differentiating amino acid substitutions to distinguish between *RPRM*, *RPRML* and *RPRM3*, we annotated *RPRM* genes in human, mouse and zebrafish. Amino acid sequences were aligned using the L-INS-i strategy from MAFFT v.7 [16]. Additionally, potential domains were predicted using the TMHMM method (http://www.cbs.dtu.dk/cgi-bin/nph-sw_request?tmhmm), as implemented in Geneious Software.

RNA extraction and reverse-transcription of cDNA templates from zebrafish larvae

For developmental expression analysis of *rprma*, *rprmb*, *rprml* and *rprm3*; embryos were collected after timed intervals of 0.2, 6, 12, 24, 31, 48, 72 and 96 hours post-fertilization (hpf), quick-frozen on liquid nitrogen, and stored at -70°C until analysis (3 independent embryo pools, 50 embryos per pool, per time point from the same spawning group). Whole embryos were homogenized in Lysis Buffer (Thermo Scientific) and total RNA was extracted with GeneJet RNA Purification kit (Thermo Scientific) according to manufacturer's instructions. Embryo *actin*, *beta 1* (*actb1*) was used for housekeeping gene expression analysis and gene of interest normalization. An aliquot (2 μl) of each extract was used for RNA quantification, quality assessment and concentration by spectrophotometry (BioSpectrometer, (Eppendorf)). RNA with a 260/280 ratio between 1.6–2.0 was considered optimal in this study. Each RNA extract was performed in triplicate and an average value was determined. cDNA was synthesized from total RNA (1 μg ; 20 μl final reaction volume) with oligo (dT) priming using ImProm-II Reverse transcriptase II (PROMEGA) according to manufacturer's instructions.

Dissection, RNA extraction and reverse-transcription of RNA templates from adult zebrafish tissues

For adult expression analysis of *rprma*, *rprmb* and *rprml*, 4 adult TAB5 wild-type male zebrafish were euthanized for organ extraction, according to the protocol by Gupta & Mullins (10.3791/1717). Zebrafish brain and bowel were harvested and homogenized in TRI-Reagent[®] (Sigma-Aldrich). Total RNA was collected separately for each sample, according to manufacturer's instructions. A 2 μl aliquot of each extract was used for RNA quantification, quality assessment and concentration by spectrophotometry (BioSpectrometer, (Eppendorf)).

cDNA was synthesized from total RNA (1 μg ; 20 μl final reaction volume) with oligo (dT) priming using ImProm-II Reverse transcriptase II (PROMEGA) according to manufacturer's instructions.

Reverse-transcription quantitative polymerase chain reaction (RT-qPCR)

All real-time PCR experiments were performed using a Stratagene Mx3000P detector system (Agilent Technologies) with optic tubes (SSI Innovations for Life Science). Amplification was achieved using Brilliant II SYBR[®] Green QPCR Master Mix (Agilent Technologies), equal amount of cDNA, and gene specific primers sets: *rprma*, fw: 5' - AACCAAACGGACAGTGGCA TCT-3', rv: 5' - AAGACTACGGTGAGGGAAAGCA-3'; *rprmb*, fw: 5' - GGCTGCAACTTGCT GATTAAGTCC-3', rv: 5' - GATGACCGCTTCCACATCCTTTGA-3'; *rprml*, fw: 5' - ACGAGCG CAAACTGTTTCGTTAC-3', rv: 5' - TCA TGAGGTTGCAGCCGAGAAA-3'; *rprm3*, fw: 5' - TG TTTCTCACGGACTACTGAACC-3', rv: 5' - TAATACGACTCACTATAGGGTGCAGCGATCAT AATAATTTCC-3'. Following completion of each real-time PCR reaction, a dissociation step was added and melt curve analysis was performed to validate the specificity of PCR amplicons. Data were processed by MxPro qPCR Software 4.10. *rprm* mRNA expression levels were normalized against an endogenous control gene previously validated as suitable reference gene for developmental studies in zebrafish [17]: *actb1*: fw: 5' - CGAGCAGGAGATGGGAACC-3', rv: 5' - CAACGGAAACGCTCATTGC-3'. Relative expression was calculated by ΔCT method against the housekeeping gene *actb1*. Expression plots were elaborated using R statistical programming language package ggplot2 and represented as average relative expression \pm SEM or relative expression boxplots, for developmental and adult expression, respectively.

Zebrafish husbandry, whole-mount in situ hybridization (WISH) and sections

Wild-type (TAB5) and transgenic reporter zebrafish (*Danio Rerio*) were maintained according to standard methods [18]. Embryos were raised in system water at 28°C and staged according to either hours post-fertilization (hpf) or morphological criteria [19]. WISH was carried out as described previously [20]. For WISH experiments, embryos older than 24hpf were treated with 0.003% 1-phenyl 2-thiourea (Sigma) to inhibit pigmentation. To better characterize the expression domains of the *rprm* genes, embryos stained with riboprobes were incubated in 30% saccharose/PBS/azide and then embedded in OCT (optimal cutting temperature) compound (Sakura). The embryos were sectioned by microtome-cryostat (Leica CM 1510S) in a series of serial transverse/coronal sections (25 μm of thickness). The sections were collected in super frost covers then dehydrated and mounted. The pictures were captured with DS-U3 Nikon camera, using the SMZ18 stereomicroscope, Nikon. All the zebrafish studies were conducted under the guidance and approval of the Institutional Animal Care and Bioethical Committee at Pontificia Universidad Católica de Chile.

cRNA probe synthesis for WISH

Templates for probe synthesis were PCR amplified from embryonic zebrafish cDNA using primers including T7 RNA polymerase promoter sequence. To minimize cross-reactivity, the 5' untranslated (5'-UTR) regions of *rprm* genes were used for primer design. Primer sets were designed as follows: *rprma*, fw: 5' - TGAGGAGAACCTCCTGTGCT-3', rv: 5' - TAA TACGAC TCACTATAGGGCCTGATCCTGATGGTTTCGT-3'; *rprmb*, fw: 5' - TCCACCCATTCATCC TGTCA-3', rv: 5' - TAATACGACTCACTATAGGGTGGAGTTTCTTCGTTTGTG-3'; *rprml*, fw: 5' - GACCGGAGATCATCCAAAGA-3', rv: 5' - TAATACGACTCACTATAGGGCTCG TTTTCGTAAACGTGCAA-3'; and *rprm3*, fw: 5' - TGTTTCTCACGGACTACTGAACC-3', rv: 5' - TAATACGACTCACTATAGGGTGCAGCGATCATAATAATTTCC-3'. All PCR products were of the expected size as inspected by agarose gel electrophoresis. Purified PCR products

were *in vitro* transcribed and labeled using digoxigenin (DIG) RNA labeling Kit (Roche) according to manufacturer's protocol. cRNA probes were purified by mini Quick Spin RNA Columns (Roche) and stored at -80°C with deionized formamide.

Fluorescent whole-mount in situ hybridization (FISH)

Embryos were fixed in 4% paraformaldehyde (PFA) in PBS at specified times post-fertilization. Samples were permeabilized with 50 µg/ml Proteinase K for 30 minutes at room temperature. Samples were then prehybridized in HYB+ with 0.1% tween SSCT at 68°C followed by incubation with antisense probes against *rprm* or *pdgfrβ* that were labeled with either Dig —or Fluorescein RNA labeling MIX (Roche) over night. Probes were detected with anti-DIG or anti Fluorescein antibody (1:500) conjugated horseradish peroxidase (Roche). Signal was produced by treatment with TSA plus Cyanine 3/Fluorescein system (PerkinElmer). Immunofluorescence was completed using rabbit anti-GFP (1:500, Life technologies), and primary antibodies were detected using anti-rabbit antibody conjugated to Alexa-488/Alexa-647 (1:500, invitrogen).

Imaging

Zebrafish embryos for WISH were embedded in 75% glycerol/PBS and imaged using NIKON eclipse 80i microscope equipped with a DS-Vi1 (NIKON) camera. Fluorescent images of embryos were acquired using Zeiss LSM780 laser-scanning confocal microscope.

Immunohistochemistry staining

Immunohistochemistry for *RPRM* (Anti-*RPRM* (38–50) antibody, Sigma-Aldrich) was performed on 4µm whole sections containing human stomach, both antral and fundic-corporal mucosa, human brain cortex, including white and gray matter, and human small bowel, obtained from the archives of the Pathology Department, Hospital Clínico Universidad de Chile, by Vectastain Elite Kit R.T.U (Vector Labs), according to manufacturer's instructions, as previously described [3]. Evaluation of immunohistochemical staining was performed independently by a pathologist (GC) who was blinded to ongoing lab results.

Results

Protein alignments

Multiple sequence alignment of *RPRM*, *RPRML* and *RPRM3* proteins between human, mouse and zebrafish showed a striking conservation of the C-terminus across species (Fig 2), while the N-terminus domain retained the most variability within the protein family. Analysis of the protein sequence by TMHMM method, revealed a short region of ~20 amino acids conforming a potential transmembrane domain in the three proteins. Amino acid differences were identified between the protein sequences, which may serve to distinguish each lineage from the others (Fig 2), colored letters in alignment; S1 Table). Aspartic acid (D), methionine (M) and glycine (G) at conserved sites serve to distinguish *RPRM* from *RPRML* and *RPRM3*. Phenylalanine (F), glycine (G) and leucine (L) at conserved sites serve to distinguish *RPRML* from *RPRM* and *RPRM3*. Aspartic acid (D), glycine (G), isoleucine (I) and leucine (L) at conserved sites serve to distinguish *RPRM3* from *RPRM* and *RPRML*. The high level of conservation (72.5% and 66% identity between human *RPRM* and zebrafish *rprma*, *rprmb* and *rprm3* proteins, respectively; 55.7% identity between human and zebrafish *RPRML* proteins) observed in the *RPRM* protein sequences and domains suggests the functions of the proteins may be related; though further research is warranted to support this conclusion.

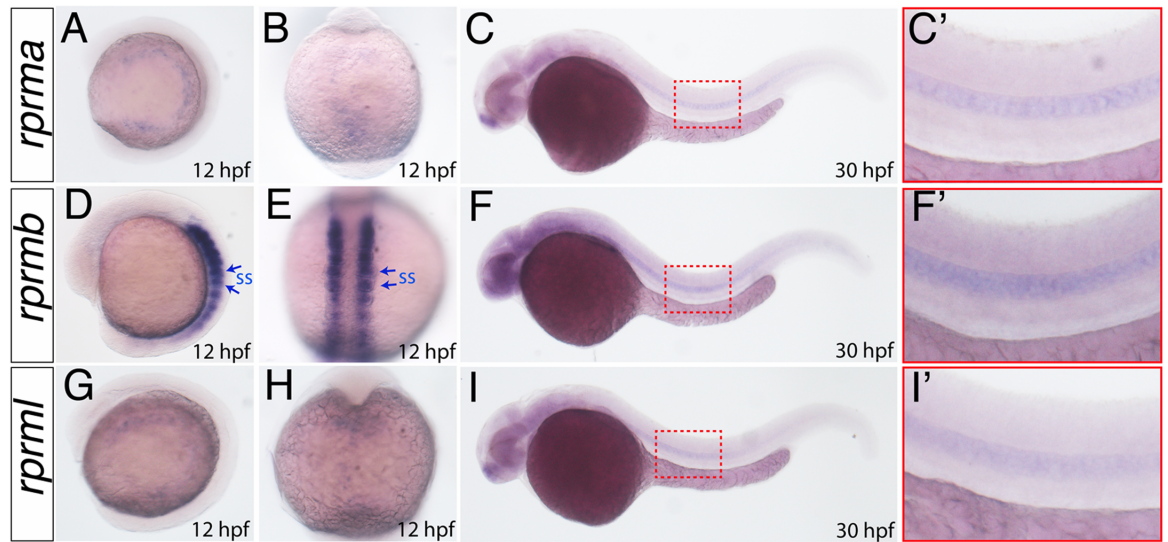


Fig 3. *rprm* expression patterns during early embryogenesis. (A-I) The expression patterns of *rprma*, *rprmb* and *rprml* were visualized by whole-mount in situ hybridization (WISH) during zebrafish embryonic development. Developmental stages are expressed as hours post-fertilization (hpf). (A, C, D, F, G, I) Lateral (anterior to the left) and (B, E, H) dorsal views are shown. Blue arrows in D-E indicate the expression in the somites (ss), while (C, F, I) the red inset magnifications indicate the expression in the notochord.

<https://doi.org/10.1371/journal.pone.0178274.g003>

(Fig 4A and 4C). *rprmb* expression was evident in two discrete domains within the preoptic region (Po) (Fig 4B) and the cranial placode in the trigeminal ganglia S4 Fig.

By 72hpf, *rprma*, *rprmb* and *rprml* maintained their expression in the fb territories (Fig 4E–4G), while *rprm3* staining was apparent in discrete regions of the midbrain (mb) (Fig 4H). We confirmed the expression of *rprma* and *rprml* in the telencephalic neurons performing whole-mount fluorescent *in situ* hybridization (FISH) (S5 Fig). In the retina, *rprma*, *rprmb* and *rprm3* positive cells were clearly expressed in the retinal ganglion cell layer (RGL) (Fig 4I), (Fig 4J and 4L). *rprml* was not expressed in the retina (Fig 4K). These results indicate that *rprm* (*rprma*/*rprmb*)/*rprml* gene expression partially overlap during zebrafish brain development. Interestingly, *rprm3*, which has been differentially retained only by some fish, showed the most unique pattern of expression in comparison to *rprm* (*rprma*/*rprmb*)/*rprml* genes during the development of the brain/CNS.

Adult zebrafish relative expression of *RPRM* transcripts within the brain was evaluated by RT-qPCR, with the exception of *rprm3* which was not assessed due the lack of this gene in humans (S6 Fig, S2 Table for raw RT-qPCR data). *rprml* showed the highest expression, followed by *rprma*. Interestingly, *rprmb* showed very low expression levels in the adult zebrafish brain S6 Fig.

Human *RPRM* protein expression was examined by immunohistochemistry (IHC) staining, using rabbit polyclonal anti-*RPRM* antibody. In the adult human brain cortex, *RPRM* protein was localized at the cytoplasm of the body and axons of neurons (Fig 4M and 4N); and at the nuclei of astrocytes (Fig 4O).

RPRM genes are expressed in zebrafish and human vascular tissues

The expression of *rprm* genes in vascular tissues begins around 48hpf. In the head, *rprm*-positive cells coat blood vessels such as central artery (CtA), primordial hindbrain channel (PHBC), mesencephalic vein (MsV), dorsal longitudinal vein (DLV), primary head sinus

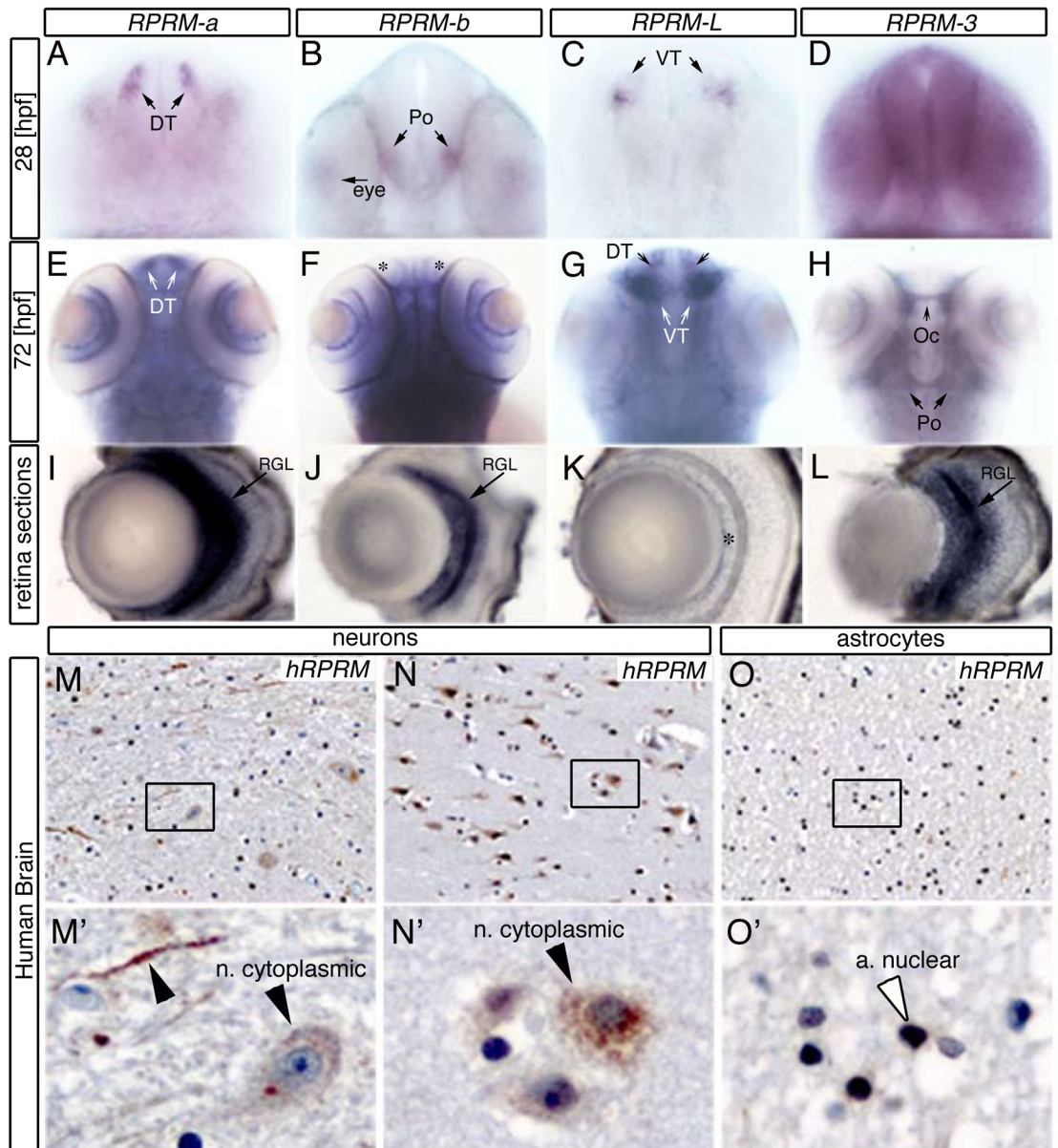


Fig 4. *RPRM* expression patterns are conserved between zebrafish and human brain. (A-D) *RPRM* expression patterns were examined using whole-mount in situ hybridization in wild-type embryos at 28 and (E-H) 72 hours post-fertilization [hpf]. (A-D) Frontal views of the embryo heads. (E-H) Dorsal views of the embryo heads. (I-L) Retina cross-sections. (A-C) At 28 hpf *rprma*, *rprmb* and *rprml* transcripts are expressed in neuronal populations such as dorsal thalamus (DT), preoptic region (Po) and ventral thalamus, respectively (black arrows). (D) *rprm3* is ubiquitously expressed throughout the brain. (E-G) At 72hpf *rprma* and *rprml* are expressed in the DT and the VT, respectively (white arrows), while *rprmb* is not expressed in those regions (asterisks). (H) At the same developmental stage, *rprm3* mRNA is expressed in the Po and the optic chiasma (Oc). (I-L) Cross sections of the retina. (I, J, L) *rprma*, *rprmb* and *rprm3* expression are restricted in the retina to the retinal ganglion cell layer (RGL, black arrow). (K) In contrast, *rprml* transcript expression is absent in the RGL (asterisk). (M, M', N, N') IHC staining for *RPRM* of white and grey matter sections from adult human samples (400x; inset magnifications 600x). (M-N) *RPRM* protein is expressed in the cytoplasm and axons of neurons (black arrowheads). (O-O') *RPRM* protein is expressed in the nuclei of astrocytes.

<https://doi.org/10.1371/journal.pone.0178274.g004>

(PHS), nasal ciliary artery (NCA) and inner optic circle (IOC) [S7 Fig](#). In addition, *rprm*-positive cells clustered together in the hypochord (Hp) posterior cardinal vein (PCV) and sprouting intersegmental vessels (ISV) [S7 Fig](#). *rprm*-positive cells were scattered throughout the brain, consistent with the possibility that *rprm* expression marks mural cells associated with the blood vessels [S7 Fig](#) (inset magnifications). To determine which cell types expressed *rprm* genes, we performed FISH followed by confocal microscopy. To visualize vasculature, we used the transgenic reporter *Tg(kdrl:EGFP)^{s843}* and *pdgfrβ*, which label vascular endothelial and mural cells, respectively [S8 Fig](#). In these experiments, we did not observe detectable co-localization. This was likely because the *rprm* genes are expressed at very low levels [S2 Fig](#). It is important to note that, despite the use of signal amplification systems for increasing sensibility, FISH detection in whole-mounts suffers for relatively low signal sensibility and signal-to-noise ratio. Thus, weakly expressed genes such as *rprms* cannot be efficiently detected.

At 72 hpf, the embryos maintained the expression of *rprma*, *rprmb* and *rprml* in brain blood vessels such as MsV, DLV and PHBC ([Fig 5A and 5C](#)). In the trunk vessels, *rprma*, *rprmb* and *rprml* transcripts were expressed at low levels in the dorsal aorta (DA), the PCV and the ISV ([Fig 5D–5F](#)). Interestingly, we did not detect vascular expression of *rprm3* during zebrafish blood vessel development (data not shown). Importantly, cells positive for *rprm* expression in vascular endothelial cells were not detected before 48 hpf ([Fig 3](#)), which indicate that *rprm* might participate in later stages of vascular commitment in the zebrafish embryos.

RPRM IHC in human samples revealed nuclear *RPRM* protein expression in endothelial cells of medium size arteries and capillaries within the wall of the digestive tube (i.e. small bowel) ([Fig 5G and 5G'](#)), as well as in the nuclei of vascular smooth muscle cells (vSMCs, also known as mural cells) of muscular arteries within the small intestine wall ([Fig 5H and 5H'](#)). The distribution observed with *RPRM* antibody was consistent with *rprm* mRNA expression during zebrafish angiogenesis.

RPRM genes are expressed in zebrafish and human digestive tract

WISH was performed to examine *rprm* gene expression in developing digestive tissues. As markers for intestinal territory, we used platelet derived growth factor beta (*pdgfrβ*) and smooth muscle alpha actin (*sm22*, also known as *transgelin1*) ([Fig 6A and 6B](#)). As the digestive organs developed, the three *rprm* (*rprma*, *rprmb* and *rprml*) genes were expressed throughout the length of the intestine. This expression pattern became increasingly prominent between 72 to 96 hpf ([Fig 6D and 6I](#)). This time period corresponds to the maturation of intestinal epithelium [21]. Of note, *rprm3* was not expressed on endoderm-derived intestinal tissues ([Fig 6C](#)). We did not detect *rprm* genes in other endoderm-derived organs such as the liver, in any stages studied.

Adult zebrafish relative expression levels of *rprm* transcripts within the intestine was evaluated by RT-qPCR [S6 Fig](#), with the exception of the *rprm3* transcript which was not expressed in this tissue, as assessed by WISH in zebrafish embryos and due to the lack of this gene in humans. Transcripts for *rprma* and *rprml* show the highest expression levels, whereas relative expression of *rprmb* was practically undetectable [S6 Fig](#).

RPRM IHC in human small bowel and stomach samples revealed expression of *RPRM* protein in the nuclei of normal enterocytes from the small bowel, especially at the base of the crypts ([Fig 6J and 6J'](#)), and in the nuclei of smooth muscle cells of the muscularis propria ([Fig 6K and 6K'](#)). *RPRM* IHC was also positive in the nuclei of normal gastric foveolar epithelium and in the nuclei of normal gastric antral and fundic glands. When compared with a recently reported work from Saavedra et al [4], in which *RPRM* expression was observed in the

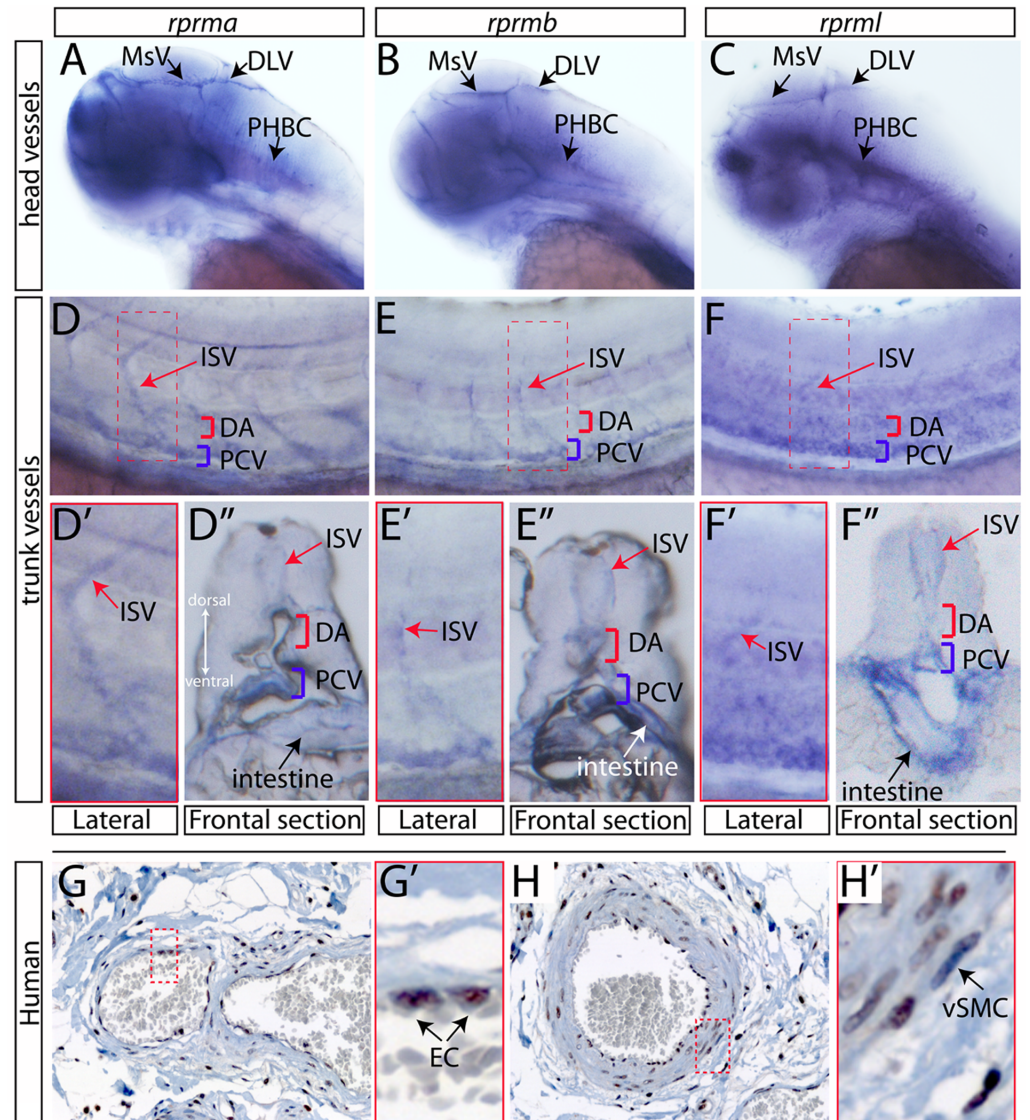


Fig 5. RPRM is expressed during zebrafish angiogenesis and in adult human vasculature. (A-C). Whole-mount in situ hybridization at 72hpf. Lateral view of the head vasculature. *rprma/b* and *l* are expressed in the mesencephalic vein (MsV), the dorsal longitudinal vein (DLV) and the primordial hindbrain channel (PHBC). (D-F) Lateral view of the trunk vessels. *rprma/b* and *l* are expressed at low levels in the dorsal aorta (DA, red bracket) the posterior cardinal vein (PCV, blue bracket) and the intersegmental vessels (ISV, red arrow). (D'-F'') Inset magnifications (red brackets) and (D''-F'') transverse histological cross-sections of the posterior trunk region. (G-H) IHC staining for RPRM in tissue sections showing small blood vessels from adult human samples (400x; inset magnification 600x). (G, G') RPRM protein is expressed in the nuclei of endothelial cells (EC, black arrows) from a small artery. (H-H') RPRM protein is expressed in the nuclei of EC and vascular smooth muscle cells (vSMCs, black arrow) of a muscular artery.

<https://doi.org/10.1371/journal.pone.0178274.g005>

cytoplasm of gastric cancer non-tumor adjacent mucosa (NTAM), only a faint positivity was observed in the cytoplasm of foveolar and antral/fundic glands epithelium.

Discussion

It has been shown that RPRM plays a critical role during carcinogenesis [4, 22–26]. Nevertheless, the expression patterns and developmental transcript localization of RPRM has not been

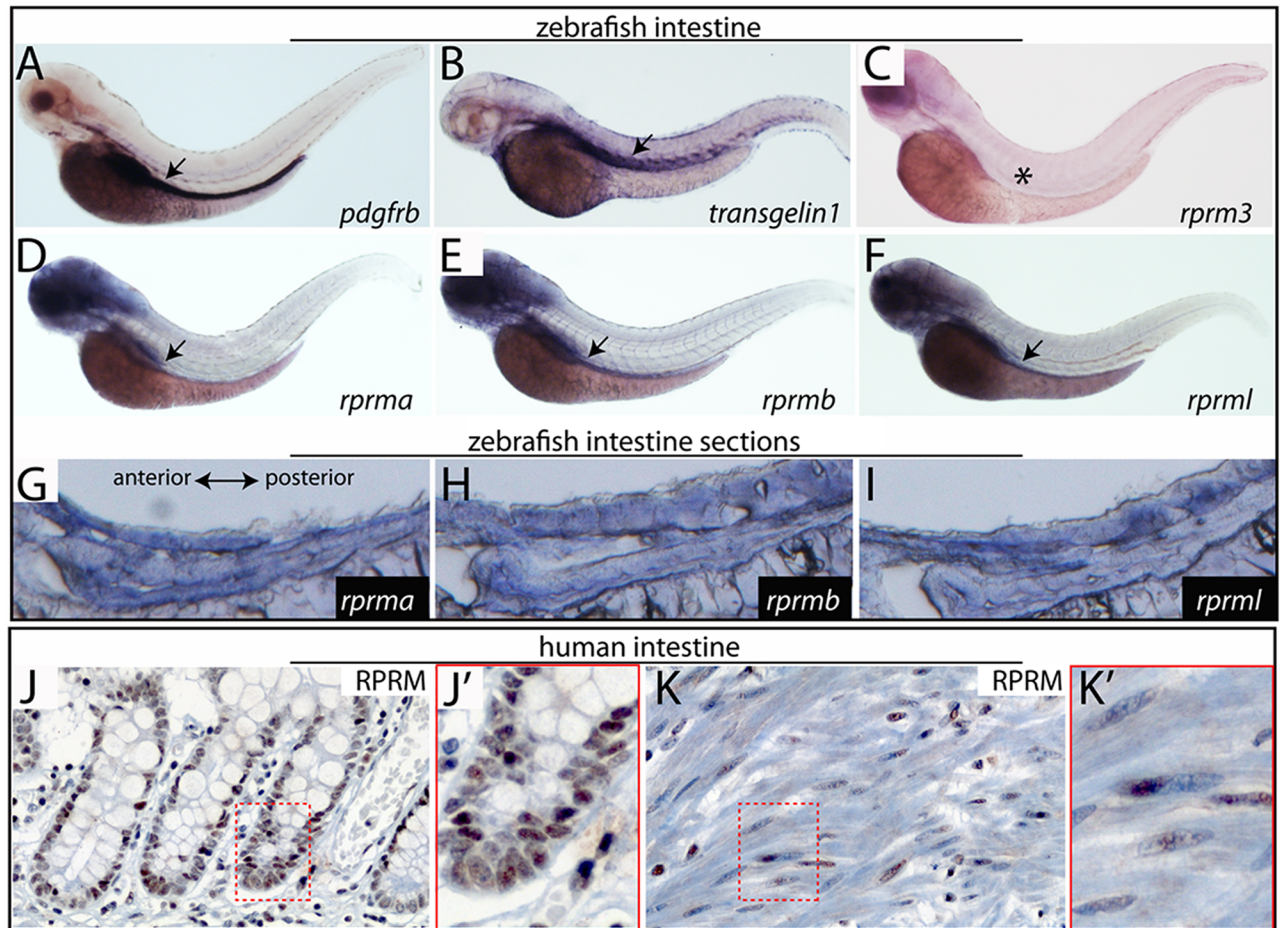


Fig 6. Expression of *rprm* genes during zebrafish gut development and human intestinal tissue. (A-F) Lateral views of whole-mount in situ hybridization (WISH) at 72hpf. (A-B) WISH for two well-known gut markers (A) platelet-derived growth factor receptor (*pdgfrβ*), (B) smooth muscle actin (*sm22*, also known as *transgelin1*), and the *rprm* genes (C) *rprm3*, (D) *rprma* (E) *rprmb* and (F) *rprml*. At 3dpf, *rprma*-b and *rprml* are expressed in the embryonic intestinal tube. At the same developmental stage, there is a lack of expression of *rprm3* in the intestinal tissue (C, asterisk). (G-I) Lateral cross sections of the zebrafish gut, anterior to the left. (J-J') *RPRM* IHC staining (400x; inset magnification 600x) showing nuclear positive expression in enterocytes at the base of the intestinal crypts. (K-K') *RPRM* IHC, (400x; inset magnification 600x) showing nuclear positive expression in smooth muscle cells from the muscularis propria of the small intestine.

<https://doi.org/10.1371/journal.pone.0178274.g006>

previously reported. Moreover, no studies have reported the transcript localization or functions of *RPRML* or *RPRM3*. In this study, we investigated for the first time the transcriptional expression profiles of *rprm* genes during zebrafish development. We used WISH to demonstrate that all of the *rprm* genes (*rprm* (*rprma/rprmb*), *rprml* and *rprm3*) were expressed during normal zebrafish embryogenesis. Gene expression profile analysis of the *rprm* genes demonstrated that they exhibit unique, although partially overlapping expression patterns during embryonic and larval development; in the brain, gut and vasculature. Most importantly, the expression patterns of *rprm* (*rprma* and *rprmb*) transcripts in zebrafish resembled human expression profiles of the *RPRM* protein product, as demonstrated by IHC staining. Note that *rprmb* is expressed primarily during developmental phases in zebrafish larvae, but expression is lost in adult zebrafish. This suggests that this duplicated gene most probably plays an important role that is restricted to development. These findings indicate that *RPRM* expression is conserved in fish and humans, subsequently validating the use of this model organism for the functional characterization of *RPRM* in development, biology and disease.

RPRM genes appear to be an evolutionary innovation of vertebrates as no traces of them have been found in urochordates. This result is in agreement with reports that suggest that a relatively high proportion of disease related genes originated in the last common ancestor of vertebrates [27]. *RPRM* genes expanded as a consequence of the two rounds of whole genome duplications that occurred early in the evolutionary history of vertebrates [28–32]. Although four gene copies are expected as a result of this process only three *RPRM* genes have been described in vertebrates to date (Fig 1; *RPRM*, *RPRML* and *RPRM3*;[1]), suggesting that one *RPRM* copy was lost shortly after a whole genome duplication event. During the evolutionary history of teleost fish (e.g. zebrafish), a third round of whole genome duplication occurred in the common ancestor of the group [33–35] that further expanded the repertoire of *RPRM* genes. The resultant *RPRM* orthologues have been differentially retained during the evolutionary history of teleosts. In the case of *RPRM*, both orthologues derived from the teleost-specific genome duplication are present in the zebrafish (*Danio rerio*) and cave fish (*Astyanax mexicanus*). For the other two *Reprimo* genes (*RPRML* and *RPRM3*), only one of the lineages has been retained. The most interesting case is the restricted phyletic distribution of *RPRM3* that among teleost fish was only identified in zebrafish and cavefish.

At the amino acid level, there is a striking conservation throughout the C-terminus of the *RPRM* family, suggesting a strong selective pressure on the composition of this domain (Fig 2). The conservation of the protein sequences between zebrafish and human *RPRM* proteins, as well as the conservation of the expression pattern of these genes, suggest that *RPRM* proteins might play homologous roles in zebrafish and humans. Therefore, zebrafish could be proposed as a model organism for the functional characterization of *RPRM* proteins.

RT-qPCR revealed the expression of *rprm* genes during embryonic development in zebrafish. *rprm* (*rprma* and *rprmb*) and *rprml* genes were detected in the forebrain and telencephalon at early developmental stages, while *rprm3* expression became progressively restricted to the midbrain (Fig 4). These genes were also detected in developing retina where they had partially overlapping expression.

In human brain, IHC staining revealed that *RPRM* was expressed in the neuronal cytoplasm and astrocyte nuclei (Fig 4). Together, the high degree of evolutionary conservation for *RPRM/RPRML* and the brain-specific expression observed between zebrafish and humans indicate that *RPRM* might be essential for brain development and/or function. Future studies using *RPRM* knockdown models will be required to determine if *RPRM* genotypic expression gives rise to a phenotype.

As in fish, human *RPRM* was expressed in the vasculature (Fig 5); specifically, in vascular smooth muscle and endothelial cells. In zebrafish, after 2dpf, the *sm22* and *acta2* label mural cells in perivascular tissues [36]. The appearance of the first *RPRM*(+)-cells in vascular tissues was observed after 2dpf (Fig 5) and S7 Fig. However, we did not observe significant fluorescent co-localization between *RPRM*(+)-cells and mural cells markers S8 Fig. Of note, fluorescent-labeled probes (FISH) are generally weaker than digoxigenin-labeled probes (WISH) for the same gene. Therefore, determining the expression pattern for particularly low-abundance transcripts such as *RPRMs* S2 Fig might not be feasible by FISH in perivascular tissues.

rprm and *rprml* expression were detected in zebrafish intestine. *RPRM* protein expression was also detected in the human gastrointestinal tract. In the latter, we observed expression of *RPRM* protein in regions of the muscularis propria surrounding the intestine (Fig 6). Histological analyses show that the zebrafish intestine is arranged in concentric smooth muscle cell layers similar to those present within the mammalian intestine [21]. This finding was consistent with previous reports indicating that the zebrafish smooth muscle layers are in correspondence with the mammalian muscularis propria [21]. In human tissue, *RPRM* protein expression was observed in the nuclei of small bowel epithelial cells, especially at the base of the crypts. *RPRM*

expression was also observed in the nuclei of human normal gastric epithelia; at foveolar epithelium and glands from the antrum and fundic regions. Interestingly, when compared with previous work of Saavedra et al [4], *RPRM* was mainly expressed in the nuclei, rather the cytoplasm, of foveolar and gastric glands epithelium, showing a faint positivity in the cytoplasm. The main difference with Saavedra et al., is that cytoplasmic *RPRM* positivity was found in gastric cancer NTAM, a mucosa with atrophy and intestinal metaplasia, both known to be premalignant lesions of the precancerous cascade of gastric cancer [37], but our case represent normal gastric human adult tissue. We speculate that *RPRM* expression and cellular location of *RPRM* may change during the precancerous cascade of gastric cancer, opening the door to future research studies.

In summary, we have isolated the *RPRM* vertebrate genes and have characterized their genetic map position, evolution and expression patterns in zebrafish and humans. Our results identify potential structural domains in *RPRM* and *RPRML* subfamilies and describe their probable evolutionary history. Taken together, the distinctive spatiotemporal localizations of the *RPRM* gene expression patterns in zebrafish suggest that these paralogs have undergone subfunctionalization through evolution. Furthermore, our evidence suggests that developmental function for the *RPRM* gene family in blood vessel formation has likely been conserved in fish and mammals. Expression during CNS formation is seen in fish and human genes throughout the *RPRM* family, suggesting a potential function in brain development which is likely ancestral to all *RPRM* genes. The developmental and cancer roles of these genes can now be tested in the zebrafish using overexpression and loss of function approaches. Therefore, zebrafish presents a unique opportunity to dissect the role of *RPRM* genes in specific cell types. Future efforts will utilize directed genomic inactivation using genome-editing technologies to better characterize this fascinating protein family.

Supporting information

S1 Fig. Patterns of conserved synteny in the genomic regions that harbor *RPRM* genes in humans and *rprma* and *rprmb* of zebrafish.

(PDF)

S2 Fig. RT-qPCR relative expression profiles of *rprm* (*rprma/rprmb*), *rprml* and *rprm3* transcripts during zebrafish development. Relative mRNA expression of *rprma*, *rprmb* and *rprml* are plotted across indicated developmental points. Each point represents the average measurement of three biological replicates. Bars correspond to standard error of the mean (SEM). Hpf: hours post-fertilization. Relative expression was normalized against *actin*, *beta 1* (*actb1*).

(PDF)

S3 Fig. Relative expression profile of *rprm* genes in embryonic zebrafish. Relative mRNA expression of *rprm* genes are plotted across indicated developmental points. Each point represents the average measurement of the relative expression of the 4 *rprm* genes (*rprma/rprmb*, *rprml* and *rprm3*). The dark grey area around the curve represents SEM.

(PDF)

S4 Fig. *rprm* expression during brain development in zebrafish embryos. *rprm* expression patterns were examined using whole-mount in situ hybridization in wild-type embryos at (A-D) 1 day post-fertilization [hpf]. (A-D) Lateral views. (A-C) At these developmental stages, *rprma*, *rprmb* and *rprml* transcripts are located in neuronal populations such as dorsal thalamus (DT), ventral thalamus (VT) and the cranial placode in the trigeminal ganglia (tg). (D)

rprm3 is ubiquitously expressed through the brain.
(PDF)

S5 Fig. *rprma* and *rprml* are expressed in brain neurons in zebrafish larvae. (A-D) *rprma* and *rprml* expression was detected by whole-mount fluorescent in situ hybridization (FISH) at 72 hours post-fertilization [hpf]. (A) Confocal cropping shows *rprma* expression in the anterior neurons of the telencephalon. (C-D) Confocal sectioning shows *rprml* expression in the posterior neurons within the forebrain (inset magnification). (A'D') Transgenic *Tg(fli1a:EGFP)* is expressed in the endothelial cells within the major blood vessels of the head.
(PDF)

S6 Fig. Relative expression of *rprm* genes in adult zebrafish brain and intestine. *rprm* genes are expressed in the brain (red dots). *rprml* and *rprma* are the highest expressed genes in the brain (red dots) and intestine (blue dots), respectively. *rprmb* has not significant expression in either tissue. *rprm3* was not included in the analysis due to the highly specific expression pattern restricted to the brain. N = 4 for each sample. Data shown as boxplots. Individual points represent relative expression (housekeeping gene used for normalization: *actb1* (β -actin)). Measurements with SD >2 from the mean expression value were considered outliers.
(PDF)

S7 Fig. *rprma* and *rprmb* are expressed during zebrafish angiogenesis. (A-B) Lateral views of whole-mount in situ hybridization at 48 hpf. *rprma/b* are expressed in the mesencephalic vein (MsV), the dorsal longitudinal vein (DLV), the primordial hindbrain channel (PHBC), the primary head sinus (PHS), the nasal ciliary artery (NCA), the primary head sinus (PHS) and inner optic circle (IOC). Inset magnification shows that *rprma/b* are expressed dispersedly throughout the head vessels. (A'-B') Lateral views of the trunk vasculature, where *rprma/b* are expressed in hypochord (Hp, black arrow), the posterior cardinal vein (PCV, white bracket) and the intersegmental vessels (ISV, white arrows).
(PDF)

S8 Fig. FISH to localize *rprm* gene expression in zebrafish larvae. Top panels showing head or trunk views. (A-B) Vascular-specific transgenic *Tg(fli1a:EGFP)* marks endothelial cells and is revealed with the anti-GFP antibody. (C-F) FISH to detect *rprma*, *rprml* and *pdgfr β* genes expression. *pdgfr β* is used as mural cell marker. (G-H) merged confocal imaging.
(PDF)

S1 Table. Differentiating elements between RPRM protein sequences. Shown are *RPRM*-, *RPRML*- and *RPRM3*-specific amino acid substitutions and positions, relative to the methionine (M) at position 1 at the N-terminus of the proteins, which are colored in Fig 2.
(PDF)

S2 Table. Raw data from RT-qPCR in adult zebrafish brain and gut.
(TXT)

Author Contributions

Conceptualization: JDA JCO AHC GIO GC RJF IAW.

Data curation: JDA JCO AHC GIO GC RJF IAW AFS ML.

Formal analysis: JDA JCO AHC GIO GC RJF IAW.

Funding acquisition: JDA JCO AHC GIO GC RJF IAW AFS ML.

Investigation: JDA JCO AHC GIO GC RJF IAW AFS ML.

Methodology: JDA JCO AHC GIO GC RJF IAW AFS ML.

Project administration: JDA.

Resources: JDA JCO AHC GIO GC RJF IAW AFS ML.

Software: JDA JCO AHC GIO GC RJF IAW AFS ML.

Supervision: JDA.

Validation: JDA JCO AHC GIO GC RJF IAW AFS ML.

Visualization: JDA JCO AHC GIO GC RJF IAW AFS ML.

Writing – original draft: JDA IAW.

Writing – review & editing: JDA JCO AHC GIO GC RJF IAW AFS ML.

References

1. Wichmann IA, Zavala K, Hoffmann FG, Vandewege MW, Corvalan AH, Amigo JD, et al. Evolutionary history of the reprimo tumor suppressor gene family in vertebrates with a description of a new reprimo gene lineage. *Gene*. 2016. <https://doi.org/10.1016/j.gene.2016.07.036> PMID: 27432065.
2. Taylor WR, Stark GR. Regulation of the G2/M transition by p53. *Oncogene*. 2001; 20(15):1803–15. <https://doi.org/10.1038/sj.onc.1204252> PMID: 11313928.
3. Ohki R, Nemoto J, Murasawa H, Oda E, Inazawa J, Tanaka N, et al. Reprimo, a new candidate mediator of the p53-mediated cell cycle arrest at the G2 phase. *J Biol Chem*. 2000; 275(30):22627–30. <https://doi.org/10.1074/jbc.C000235200> PMID: 10930422.
4. Saavedra K, Valbuena J, Olivares W, Marchant MJ, Rodriguez A, Torres-Estay V, et al. Loss of Expression of Reprimo, a p53-induced Cell Cycle Arrest Gene, Correlates with Invasive Stage of Tumor Progression and p73 Expression in Gastric Cancer. *PLoS One*. 2015; 10(5):e0125834. <https://doi.org/10.1371/journal.pone.0125834> PMID: 25954972
5. Buchegger K, Ili C, Riquelme I, Letelier P, Corvalan AH, Brebi P, et al. Reprimo as a modulator of cell migration and invasion in the MDA-MB-231 breast cancer cell line. *Biol Res*. 2016; 49:5. <https://doi.org/10.1186/s40659-016-0066-7> PMID: 26796959
6. Garcia-Bloj B, Moses C, Sgro A, Plani-Lam J, Arooj M, Duffy C, et al. Waking up dormant tumor suppressor genes with zinc fingers, TALEs and the CRISPR/dCas9 system. *Oncotarget*. 2016; 7(37):60535–54. <https://doi.org/10.18632/oncotarget.11142> PMID: 27528034.
7. Bernal C, Aguayo F, Villarroel C, Vargas M, Diaz I, Ossandon FJ, et al. Reprimo as a potential biomarker for early detection in gastric cancer. *Clin Cancer Res*. 2008; 14(19):6264–9. <https://doi.org/10.1158/1078-0432.CCR-07-4522> PMID: 18829507.
8. Portela A, Esteller M. Epigenetic modifications and human disease. *Nature biotechnology*. 2010; 28(10):1057–68. <https://doi.org/10.1038/nbt.1685> PMID: 20944598.
9. Sato N, Fukushima N, Matsubayashi H, Iacobuzio-Donahue CA, Yeo CJ, Goggins M. Aberrant methylation of Reprimo correlates with genetic instability and predicts poor prognosis in pancreatic ductal adenocarcinoma. *Cancer*. 2006; 107(2):251–7. <https://doi.org/10.1002/cncr.21977> PMID: 16752411.
10. Ooki A, Yamashita K, Yamaguchi K, Mondal A, Nishimiya H, Watanabe M. DNA damage-inducible gene, reprimo functions as a tumor suppressor and is suppressed by promoter methylation in gastric cancer. *Mol Cancer Res*. 2013; 11(11):1362–74. <https://doi.org/10.1158/1541-7786.MCR-13-0091> PMID: 23982217.
11. Howe K, Clark MD, Torroja CF, Torrance J, Berthelot C, Muffato M, et al. The zebrafish reference genome sequence and its relationship to the human genome. *Nature*. 2013; 496(7446):498–503. <https://doi.org/10.1038/nature12111> PMID: 23594743.
12. White R, Rose K, Zon L. Zebrafish cancer: the state of the art and the path forward. *Nat Rev Cancer*. 2013; 13(9):624–36. <https://doi.org/10.1038/nrc3589> PMID: 23969693.
13. MacRae CA, Peterson RT. Zebrafish as tools for drug discovery. *Nat Rev Drug Discov*. 2015; 14(10):721–31. <https://doi.org/10.1038/nrd4627> PMID: 26361349.
14. Serbedzija GN, Flynn E, Willett CE. Zebrafish angiogenesis: a new model for drug screening. *Angiogenesis*. 1999; 3(4):353–9. PMID: 14517415.

15. Tobia C, De Sena G, Presta M. Zebrafish embryo, a tool to study tumor angiogenesis. *The International journal of developmental biology*. 2011; 55(4–5):505–9. <https://doi.org/10.1387/ijdb.103238ct> PMID: 21858773.
16. Katoh K, Standley DM. MAFFT multiple sequence alignment software version 7: improvements in performance and usability. *Molecular biology and evolution*. 2013; 30(4):772–80. <https://doi.org/10.1093/molbev/mst010> PMID: 23329690.
17. McCurley AT, Callard GV. Characterization of housekeeping genes in zebrafish: male-female differences and effects of tissue type, developmental stage and chemical treatment. *BMC molecular biology*. 2008; 9:102. <https://doi.org/10.1186/1471-2199-9-102> PMID: 19014500.
18. Westerfield M. *The zebrafish Book*, 3rd ed. University of Oregon Press, Eugene, OR. 1995.
19. Kimmel CB, Ballard WW, Kimmel SR, Ullmann B, Schilling TF. Stages of embryonic development of the zebrafish. *Dev Dyn*. 1995; 203(3):253–310. <https://doi.org/10.1002/aja.1002030302> PMID: 8589427.
20. Amigo JD, Ackermann GE, Cope JJ, Yu M, Cooney JD, Ma D, et al. The role and regulation of friend of GATA-1 (FOG-1) during blood development in the zebrafish. *Blood*. 2009; 114(21):4654–63. <https://doi.org/10.1182/blood-2008-12-189910> PMID: 19729519.
21. Wallace KN, Akhter S, Smith EM, Lorent K, Pack M. Intestinal growth and differentiation in zebrafish. *Mechanisms of development*. 2005; 122(2):157–73. <https://doi.org/10.1016/j.mod.2004.10.009> PMID: 15652704.
22. Ellinger J, Bastian PJ, Jurgan T, Biermann K, Kahl P, Heukamp LC, et al. CpG island hypermethylation at multiple gene sites in diagnosis and prognosis of prostate cancer. *Urology*. 2008; 71(1):161–7. <https://doi.org/10.1016/j.urology.2007.09.056> PMID: 18242387.
23. Hamilton JP, Sato F, Jin Z, Greenwald BD, Ito T, Mori Y, et al. Reprimo methylation is a potential biomarker of Barrett's-Associated esophageal neoplastic progression. *Clin Cancer Res*. 2006; 12(22):6637–42. <https://doi.org/10.1158/1078-0432.CCR-06-1781> PMID: 17121882.
24. Luo J, Zhu Y, Yang G, Gong L, Wang B, Liu H. Loss of Reprimo and S100A2 expression in human gastric adenocarcinoma. *Diagn Cytopathol*. 2011; 39(10):752–7. <https://doi.org/10.1002/dc.21461> PMID: 20949468.
25. Nakajima T, Yasufuku K, Suzuki M, Fujiwara T, Shibuya K, Takiguchi Y, et al. Assessment of Chemosensitivity-related Aberrant Methylation of Nonsmall Cell Lung Cancer by EBUS-TBNA. *J Bronchology Interv Pulmonol*. 2009; 16(1):10–4. <https://doi.org/10.1097/LBR.0b013e318195d930> PMID: 23168460.
26. Nishida N, Nagasaka T, Nishimura T, Ikai I, Boland CR, Goel A. Aberrant methylation of multiple tumor suppressor genes in aging liver, chronic hepatitis, and hepatocellular carcinoma. *Hepatology*. 2008; 47(3):908–18. <https://doi.org/10.1002/hep.22110> PMID: 18161048.
27. Maxwell EK, Schnitzler CE, Havlak P, Putnam NH, Nguyen AD, Moreland RT, et al. Evolutionary profiling reveals the heterogeneous origins of classes of human disease genes: implications for modeling disease genetics in animals. *BMC evolutionary biology*. 2014; 14:212. <https://doi.org/10.1186/s12862-014-0212-1> PMID: 25281000.
28. Meyer A, Schartl M. Gene and genome duplications in vertebrates: the one-to-four (-to-eight in fish) rule and the evolution of novel gene functions. *Current opinion in cell biology*. 1999; 11(6):699–704. PMID: 10600714.
29. McLysaght A, Hokamp K, Wolfe KH. Extensive genomic duplication during early chordate evolution. *Nature genetics*. 2002; 31(2):200–4. <https://doi.org/10.1038/ng884> PMID: 12032567.
30. Dehal P, Boore JL. Two rounds of whole genome duplication in the ancestral vertebrate. *PLoS biology*. 2005; 3(10):e314. <https://doi.org/10.1371/journal.pbio.0030314> PMID: 16128622.
31. Hoegg S, Meyer A. Hox clusters as models for vertebrate genome evolution. *Trends in genetics: TIG*. 2005; 21(8):421–4. <https://doi.org/10.1016/j.tig.2005.06.004> PMID: 15967537.
32. Putnam NH, Butts T, Ferrier DE, Furlong RF, Hellsten U, Kawashima T, et al. The amphioxus genome and the evolution of the chordate karyotype. *Nature*. 2008; 453(7198):1064–71. <https://doi.org/10.1038/nature06967> PMID: 18563158.
33. Meyer A, Van de Peer Y. From 2R to 3R: evidence for a fish-specific genome duplication (FSGD). *BioEssays: news and reviews in molecular, cellular and developmental biology*. 2005; 27(9):937–45. <https://doi.org/10.1002/bies.20293> PMID: 16108068.
34. Kasahara M. The 2R hypothesis: an update. *Current opinion in immunology*. 2007; 19(5):547–52. <https://doi.org/10.1016/j.coi.2007.07.009> PMID: 17707623.
35. Opazo JC, Butts GT, Nery MF, Storz JF, Hoffmann FG. Whole-genome duplication and the functional diversification of teleost fish hemoglobins. *Molecular biology and evolution*. 2013; 30(1):140–53. <https://doi.org/10.1093/molbev/mss212> PMID: 22949522.

36. Santoro MM, Pesce G, Stainier DY. Characterization of vascular mural cells during zebrafish development. *Mechanisms of development*. 2009; 126(8–9):638–49. <https://doi.org/10.1016/j.mod.2009.06.1080> PMID: 19539756.
37. Correa P, Piazeulo MB. The gastric precancerous cascade. *Journal of digestive diseases*. 2012; 13(1):2–9. <https://doi.org/10.1111/j.1751-2980.2011.00550.x> PMID: 22188910.
38. Hedges SB, Marin J, Suleski M, Paymer M, Kumar S. Tree of life reveals clock-like speciation and diversification. *Molecular biology and evolution*. 2015; 32(4):835–45. <https://doi.org/10.1093/molbev/msv037> PMID: 25739733.